

We are IntechOpen, the world's leading publisher of Open Access books Built by scientists, for scientists

6,900

Open access books available

185,000

International authors and editors

200M

Downloads

Our authors are among the

154

Countries delivered to

TOP 1%

most cited scientists

12.2%

Contributors from top 500 universities



WEB OF SCIENCE™

Selection of our books indexed in the Book Citation Index
in Web of Science™ Core Collection (BKCI)

Interested in publishing with us?
Contact book.department@intechopen.com

Numbers displayed above are based on latest data collected.
For more information visit www.intechopen.com



Principles and Thermo-Mechanical Model of Friction Stir Welding

Jauhari Tahir Khairuddin, Jamaluddin Abdullah, Zuhailawati Hussain and Indra Putra Almanar

Additional information is available at the end of the chapter

<http://dx.doi.org/10.5772/50156>

1. Introduction

Friction stir welding (FSW) is a solid-state welding process that gained much attention in research areas as well as manufacturing industry since its introduction in 1991 [1, 2]. For almost 20 years, FSW has been used in high technology applications such as aerospace to automotive till high precision application such as micro welding. The main feature of a solid-state welding process is the non-melting of the work material which allows a lower temperature and a lower heat input welding process relative to the melting point of materials being joined. This is advantageous over the conventional fusion welding where excessive high heat input is required to melt the work material. Much less heat input required for FSW translates into economic benefits, safer and less complicated welding procedures. The friction stir welding make it possible to join light weight materials such as aluminium alloy, magnesium alloy, copper and titanium alloys which are very difficult to weld by conventional welding. These clear advantages have greatly increased the usage of these materials in structural applications [3, 4]. In addition, FSW also makes possible to produce sound weldment in 5000 and 7000 series aluminium alloys that are not possible to be welded using conventional method. FSW does not produce sparks or flames. Thus, safety, environmental and legislation issues are not of major concern. FSW process provides proven good quality and strong weldment with inexpensive and lesser number of equipment, eliminates the use of filler metal and improved weldability. Due to these factors FSW has successfully been employed in aerospace, automobile and ship building industries. The need to further understand and improve FSW process continues to propagate in many applications. Many researchers have looked into several methods including mathematical modelling of the process, aiming at understanding the physical-material interaction [8 – 14]. However, there is lack of recorded work in the literature on a system or method to quantitatively measure the welding parameter such as force and torque in FSW process.

This chapter aims to introduce FSW process, its parameters, the applications and a thermo-mechanical model of the process. From the mathematical model derived, a measurement apparatus was developed for force and torque determination during FSW process and experiments were performed to validate the model.

2. Friction stir welding process

FSW set up consists of (1) cylindrical rotational tool, (2) two or more work materials of similar or dissimilar material combinations (3) backing plate and finally (4) clamping or holding fixture as shown in figure 1.

The rotating tool design consists of a combination of two cylinders of a specific radius ratio known as shoulder and smaller radius pin or probe, where the height of the pin or probe is usually more than half of the work material thickness but not equal to its overall thickness. The work materials to be joined may be arranged as conventional welding method but the most common configurations used in FSW are abutted and lapped configuration. For any configuration, FSW has the capability to join thick plate without the need for special preparation prior to welding process. Meanwhile, the backing plate is to ensure the establishment of confine volume and it becomes a must when welding with a pin penetration approaching the bottom of the work materials. The most crucial part of the work materials set up is the clamping or holding fixture. Improper clamping may jeopardize the mated surfaces to be welded and will generate gaps leading to the formation of worm hole or cavities in the weldment. FSW is the non-filler process; hence no substitute material to fill in gaps created by the separation of the work materials is required.



Figure 1. Friction stir welding experimental set up [5].

2.1. Stages in friction stir welding process

FSW process involves four phases which are (1) plunging phase, (2) dwelling phase, (3) welding phase, and finally (4) exit or retract phase. Briefly, the process starts with rotating tool pin or probe thrusting onto the configured work materials under a constant axial load to generate friction heat. This process will continuously increase the temperature at the immediate contacting surface of the rotating tool and work material. The process continues until the temperature at the immediate contact of the rotating tool and the work material increased to a temperature which causes the work material to soften, plasticized and significantly lose its strength. Consequently, these conditions allow the rotating tool to penetrate to a certain depth usually almost to the thickness of work material. The plasticized material is subjected to displacement by the rotating tool pin plunge, effectively being flashed out with a portion of the generated heat, thus introducing new immediate lower temperature and harder surface of work material. This event explains the transient heat generated through pure mechanical friction work at the tool and work material interface. The end of the plunging phase is signified by the sound contact of the rotating tool shoulder with the immediate work material surface.

At this moment, the process enters the dwelling phase where the rotating tool is allowed to dwell for a period of time, causing the temperature to increase further, up to its hot working temperature. The heat generated from frictional work is greatly dependent on the relative increase of contact surface area as well as the relative speed. The heat generated causes the affected area under the shoulder to expand considerably. Phenomenally, the heat causes the work material close to the immediate contact to lose its strength and become plastic. Once this condition is reached, thin soft material layers are produced and would stick to the dynamic rotating tool surfaces (pin and shoulder) and being forced to be displaced along. Instantly the mechanical friction heat generation is partially turned into plastic dissipation heat generation. It is explained by the energy dissipated from the internal shearing of different velocity between the displaced softened work material layers to static more solid surface. Ideally, intermittent heat generation mechanisms due to friction work and plastic dissipation take place because of the transient heat transfer effect and the material ability to regain its strength as heat is lost to the ambient. In addition, the other role of these frictional work and plastic deformation mechanisms are to induce soft material displacement and causes the stirring action or severe material deformation which later produce the amalgamated joint.

The dwelling phase is followed by welding phase. After the local temperature of work material under the rotating tool approaches its hot working temperature and is soft enough to be stirred and displaced, the rotating tool is moved transversely along the welding line. This traverse motion causes the plasticized soft material at the leading edge of the rotating tool being squeezed and sheared through a small slit formed by the displaced soft material at the side or lateral of the tool, preferably in the direction of tool rotation. The displaced soft material is then deposited to the gap at the trailing edge left by rotating tool pin or probe. The soft plasticized material is forcibly displaced by the rotating tool along its rotating

direction under a closed encapsulation of harder solid work material wall and rotating tool shoulder. The soft material is forged to the trailing edge in layers, forming weld nugget. At each traverse increment of the rotating tool motion, the displacement of soft plasticized work material to the trailing edge will introduce new solid, lower temperature work material at the leading edge. Thus it reintroduces friction work heat generation mechanism prior to plastic deformation mechanism and continuously repeating the heat generation process all over again at each traverse displacement of the tool. This produces cyclic transient heat generation. This cyclic process takes part throughout the welding phase and strongly affected by the combination of the rotating tool's rotational and traverse speed. Recap, during the welding phase the plasticized material is subjected to displacement, extrusion and shearing mechanisms facilitated by the tool rotation, thrust and transverse movement under cyclic heat generation along welding line and finally consolidating welding nugget in the trailing side.

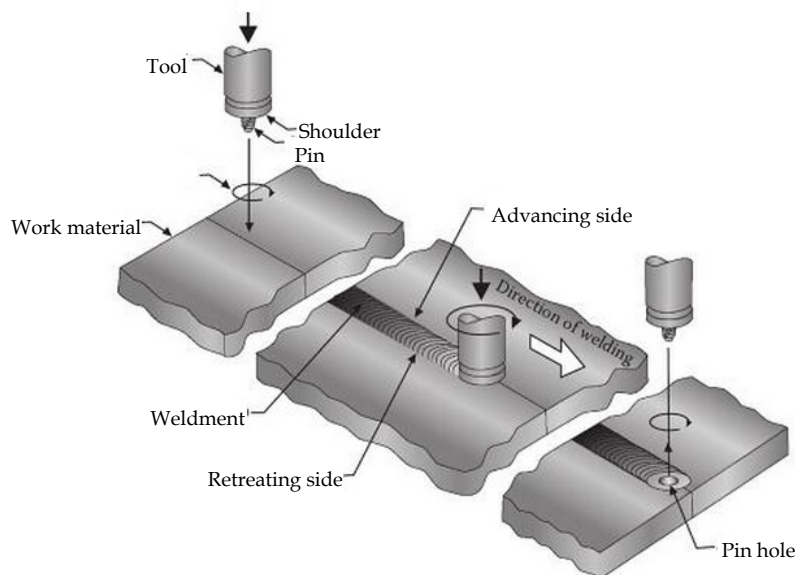


Figure 2. Friction Stir welding process phases of a butted work material configuration [6].

At the end or exit phase of FSW process, the rotating tool is retracted away from the work material leaving a cylindrical hole mark that once occupied by the tool pin. For cosmetic reason, the cylindrical hole may be filled with filler material at the end of the welding process but the most common method used is by introducing dummy material prior the exit phase. Dummy material is of the same material used for the work material to be weld and placed at the end of welding line where the rotating tool is allowed to traverse to and exit within it. The dummy material is later to be cut away leaving good surface finish. Though, this cosmetic issue would remain in the application of innovated friction stir spot welding.

These process phases in FSW are dependent to one another to produce a good amalgamated weldment and are strongly affected by the welding parameters. The assurance of good weldment is determined by proper control of varying measureable welding parameters such as rotational speed, axial plunge force and torque, traverse speed, tool geometry and

orientation in the form of heat energy. Similar to other conventional welding methods, heat energy notably determines the quality of the joint.

2.2. Thermo-mechanical dynamic of friction stir welding

To understand the working principle of friction stir welding, it is necessary to explore the physics related to heat generation. Friction stir welding process started with initial mechanical friction between tool and the surface to be welded which results in heat generation. Rotating tool rotates and advances in trust motion against the work material followed by heat generated through plastic dissipation or deformation of sheared and strained layers of soften material close to the rotating tool surfaces. The heat generation mechanisms occur intermittently or in cycle throughout the welding process.

2.2.1. Friction heat generation

Mechanical friction work is initiated when rotating tool surfaces are in contact with the immediate stationary surface of work material under a normal load. While the rotating tool is sliding, it introduces velocity difference between the dynamic rotating tool and the static work material surface and thus creates friction work and subsequently, heat. This mechanical friction work is described based on the Amonton's laws which firstly explain that the friction between two separate bodies is directly proportional to the normal load applied onto the bodies. In this law, coefficient of friction of static friction is a constant variable and temperature dependent but only to be considered as kinetic friction when the contact condition is non-sticking or sliding. Secondly, the friction force is independent on the apparent contact area [7].

In general application, friction work is assumed based on Coulomb's dry friction model between solid bodies, which is also at the same time conforms the aforementioned Amonton's law. In details, the mechanical work and heat generation relationship in the presence of sliding friction is explained by contact conditions between hard and soft metallic material interaction. It involves very small scale asperities at the contact surfaces of hard and soft material. As normal force is acting on the rotating tool, it is being distributed onto smaller area asperities at the contact surfaces which resulted in a very high pressure per unit force. Due to relative velocity difference, the normal force causes ploughing of the soft material by the hard materials' asperities. The soft material gets agitated, deformed and finally broken, releasing the stored energy in the form of heat [8].

The released energy which is a very high local thermal energy causes the temperature to rise. The heat energy is eventually transferred and stored into the rotating tool and the lump work material. The heat causes the work material to soften, reduces its strength, broken and deforms into soft material layer in between the rotating tool and the work material. This soft layer is gradually displaced by the rotating tool pin revealing new surface contact condition for another cycle of ploughing action by the rotating tool. The process promotes another cycle of mechanical friction heat generation.

2.2.2 *Plastic dissipation heat generation*

This phenomenon typically occurs at higher temperature resulting from friction heat mechanism but only significant during dwelling and actual welding phase where work material is confined under the rotating tool. Through friction heat mechanism, work material temperature under the rotating tool is increased to a degree where work material layer at rotating tool interface started to lose its strength, yielded, stick and move with the rotating tool. This phenomenon increases the thermal softening effect from friction heat and causes shears at the work material to work material layers interface. It reduces friction heat mechanism but at the same time introduce high strain rate plastic deformation. As a result, highly localized heat is generated internally within the work material itself away from the rotating tool to work material interface due to dynamic velocity differences and boundary sliding condition [9, 10, 11].

Due to the heat transfer within the process, the plastically deformed material tend to recover its strength thus establishing new lower temperature level and reinitiate mechanical friction heat generation mechanism [12]. Furthermore at the welding phase, heat generation from plastic dissipation mechanism is increased at cost of the travelling rotating tool and the shearing of the work material to higher extend toward trailing edge. It further increases the process temperature as the rotating tool is reintroduced to new contact condition at the leading edge and reinitiates the mechanical friction heat generation mechanism [13].

These heat generation mechanisms throughout FSW process occur in cycles due to the instance of slip and stick contact conditions and the alternating boundary conditions at the material-rotating tool interface [14]. In this regards, heat generation mechanism has most influential effects on the process introducing high strain rate and thermal effect which soften work material adjacent to the tool to work material interface, to be encompassed the at the trailing edge and produces welding nugget which posture the main characteristic of the joint [15].

2.2.3. *Heat transfer*

Simultaneously, heat generated is constantly being transferred within the system; portions of heat are distributed within the work material, the rotating tool, the holding fixture or backing plate and finally to the ambient. In depth, heat generated is subjected to three dimensional (3-D) heat flows away from the heat source under boundary conditions. Heat input and heat transfer at the rotating tool are indirectly coupled at the rotating tool to work material interface into the work material through heat conduction and incorporated with convective heat transfer effect around the pin in the deformation zone [12, 13, 16, 17]. For the work material, convective and radiative heat transfers are considered for heat exchange at the top work material surface, past the shoulder peripheral while at the same time only convective condition is considered for the bounding surfaces of work material [18, 19]. For the case of backing plate, appropriate variable gap conductance is considered for work material to backing plate interface depending on specific thermal contact resistance condition; of temperature dependent or contact pressure dependent or surface contour of work material or any of the combinations [13, 18, 20].

Ultimately 100% energy generated from mechanical work throughout the process is converted to heat and physical deformation with approximately 88% of heat is conducted and distributed globally through to the lump work material, backing plate and else to the rotating tool [12]. Heat plays a very significant role not only toward the physical success of the joint but also towards the process temperature profile, heat transfer and the work material internal strain and stress distribution. It causes direct influences on the final weldment microstructure and residual stress resulting properties which are strongly correlated to the welding variables and temperature-dependent material properties [21].

2.2.4. Friction stir welding mechanism

Weldment is produced in the course of welding phase where layers of materials are forced to move along with and around the rotating tool surfaces at a specific contact condition; fully sliding or sliding and sticking or fully sticking. The soft material layers motion are heavily deformed and driven by the tool rotational direction. It is forced through the retreating side toward trailing edge and downward closed to the pin before finally being forged and deposited at the once occupied volume of the rotating tool pin at the trailing edge under severe plastic deformation [17, 21, 22, 23].

The mechanical torque of the rotating tool causes mechanical shearing to the immediate work material close to the rotating tool and work material interface, forcing soft work material layers to motion and strained, creating flows of fine layers of materials prior progression into weldment. The flow motion or velocity is visually estimated through the grain size and shape, correlated to internal strain rate [24]. The material flow and joining mechanisms are described by the region formed by the FSW process known as the flow zones. It describes the zones where shear layers are visibly distinguished by material characteristics and exhibit the evident of non-melting but severely deformed soft material deposited into amalgamated weldment in layers and flowing manner.

2.2.5. Welding characteristics

Temperature profile and history of FSW process are resembled by the distinct regions at the weldment. These regions are characterized by discrete microstructure sizes, shapes and varying properties, produced by the significant thermal effect and mechanical deformation. Under the heat generation, lump effect and heat transfer of the process, thermal profiles are being distributed from the crown shaped heat source around the rotating tool to work material interface toward the peripheral work materials surfaces and edges [22, 25]. These regions are known as; 1) weld nugget, the product of plastic deformation due to the stirring effect deposited behind the rotating tool pin at the trailing edge, 2) thermo-Mechanically Affected Zone (TMAZ) of internally sheared plastic deformation within the work material away from rotating tool to work material interface, 3) heat Affected Zone (HAZ) of structurally altered and thermally affected region due to intense temperature different between TMAZ and base metal temperature region, and 4) base metal of work material which is not physically affected by the thermal effect [26].

Temperature profile within the FSW process portrayed direct relationship of the heat generation, torque generated through the rotating tool, loads exerted throughout the work material and power consumed by the welding process. Both thermal and mechanical effect from heat generation and stirring effect engender welding characteristic in term of stresses, tensile and hardness properties. For which, the rotating tool rotational and traverse speed interchangeably influenced the temperature profile and affectively manipulate the material flow behaviour, weld material chemical composition, microstructure orientation, strain, residual stress, thermal stress, material hardness and strength of the weldment [27, 28, 29]

2.3. Applications of friction stir welding

Recently, FSW won attractive attention by manufacturing industries because of the ability that outperformed other welding technique such as tungsten inert gas (TIG) to weld aluminium. Besides, it has the ability to be adapted in advanced automation system such as robotic which is very predominant in aluminium components and panel fabrications of highly rated technology readiness level [30]. For example, it is an applicable technique adapted for rail cars for fabrication of floor panel part of a Type 700 Shinkansen or bullet train, as well as the aluminium roof, side wall and floor panel for suburban train and other more recent commuter or express rail cars [31]. This is due to its low distortion and its suitability to produce large welded products including prefabricated panels as well as tailored blanks and joints. These advantages are also shared in marine application when it is first commercially used for ship building in 1996 with the ability to joint thick panels, sandwiched, honeycomb panels and corrosion resistance material panels [32]. FSW is well favoured for performing butt joint in comparison to conventional arc welding application which also turns out to be significantly viable in terms of low labour cost and shorter welding cycle time [33].

The other important application of friction stir welding is in aeronautical and aerospace industries where aluminium alloy is used as primary material for their construction. The welding process enables manufacturers to completely replace the riveted joints and assemblies of lapped and abutted configuration that are used mainly for fuselage sections, propellant and fuel tanks of commercial air craft as well as space launch vehicle [34]. Thus, the process allows total elimination of the use of thousands of rivets. This has resulted in better quality, stronger and lighter joints at reduced assembly cost for aviation industry. Meanwhile in automotive application, FSW and its recently innovated process of friction stir spot welding (FSSW) are introduced to replace conventional resistive spot welding (RSW) in the transition when aluminium alloy application is ready and becoming ideal to be used for panels in passenger and commercial vehicle bodies. Aluminium application in automotive industry are sought for its prefabricated and tailored panel, good strength-to-weight ratio, potential for reducing fuel consumption, its ease of recycling as well as marked reduction in production cost. This has compelled car manufacturers to use the same concept not only for the body panels, but for other parts as well [35].

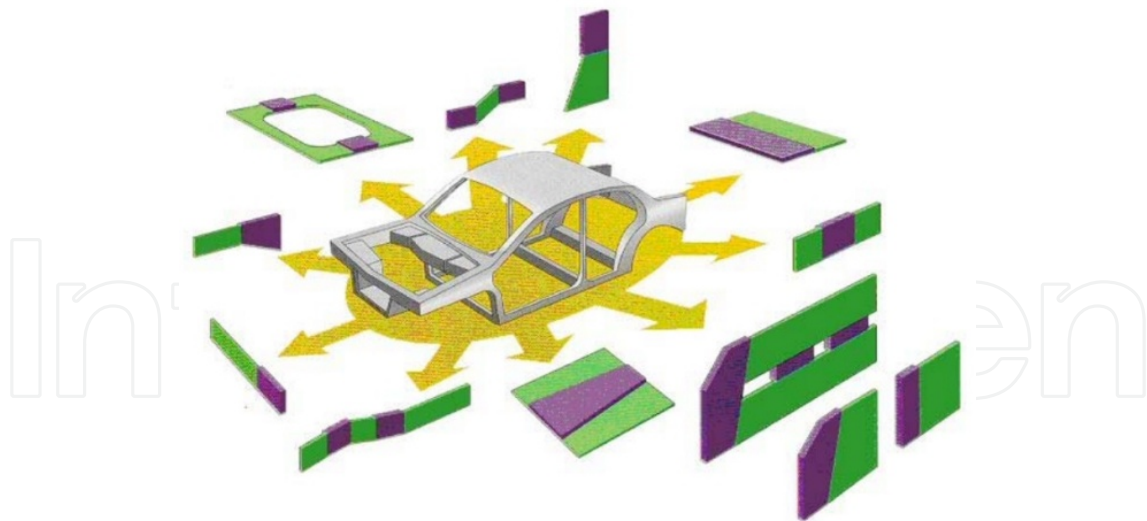


Figure 3. Tailored welded blanks in a passenger vehicle [36].

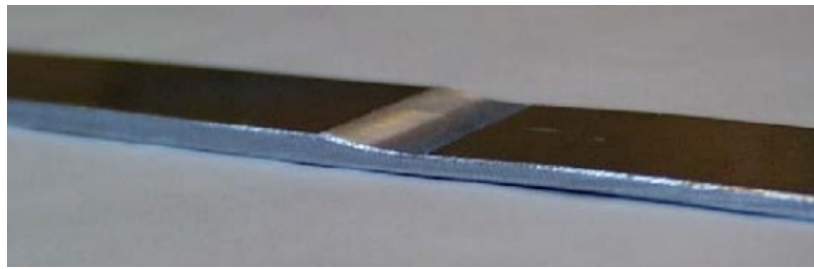


Figure 4. A component of friction stir tailored welded blank [36].

Since its introduction, friction stir welding has matured significantly with widespread use of wide range aluminium alloys for structural applications with its compatibility to be used in ferrous, stainless steel, nickel, copper and titanium alloys. However, only a small percentage of world welding and joining market has implemented the process. It is still relatively underutilised and this is varied among industries, university researches, collaborations and other niche applications. With all the challenges to joints wide variety hard to weld materials, the motivation of the application and adaptation of this noble technology in manufacturing not only to meet quality joints, but for the potential economic value and also for its environmental friendliness.

2.4. Recent development & future outlook

Since the last two decades, there are considerably vast lab and industrial work done on FSW process which leads to the emerging advancement of new materials application and combinations, process improvement, tool designs, welding configurations, tailored blank application and adaptation to automation. Though, the most important innovation in the process itself is its variations; (1) high speed FSW (HS-FSW), (2) ultrasonic stir welding (USW), (3) thermal stir welding (TSW), (4) friction stir spot welding (FSSW), (5) friction stir joining (FSJ), (6) friction stir processing (FSP), (7) friction bonding (FB) [37].

The recent advancement shows the introduction of HS-FSW aiming at reducing the process forces by means of increasing heat generation rate. This reduction in forces is to realize the idea of permitting manual handheld welding work. HS-FSW process is also designed to achieve lighter and portable device or equipment. This will make possible manual handheld welding and eliminates the need for rigid fixturing of the work material and rotating tool.

USW is another variation of the process where ultrasonic energy is used to assist in initial heat generation. The objectives are to reduce process forces and welding time. The major boost of USW is it reduces dependency on the tool shoulder to generate heat and instead, make use of the coupled ultrasonic vibration to further agitate the rotating tool at the contact interface, amplifying the mechanical friction effect.

Different from USW that utilize ultrasonic energy to generate heat, TSW decouples heat generation from mechanical friction of conventional FSW and instead, utilizes external induction heating to increase work material temperature at the welding spot or welding line. Though induction heating may ultimately increase the rate of heat generation but it reduces strain rate of plastic deformation, a prevalent characteristic in FSW. Reduced strain rate will significantly affect the final welding properties [38].

The most common variation of all is the FSSW, which is well known to be used in transportation industries to replace rivet and as well as adhesive joining method. Though this method produces cosmetic defect in the form of pin hole created by the rotating tool, the weldment has sufficient mechanical strength for joining method [39].

While the other FSW variants are dedicated for metallic materials, FSJ method is dedicated for joining thermoplastic materials. It has been used for polypropylene, polycarbonate and high density polyethylene materials [40]. The advancement of FSJ method may possibly makes way for mechanical joining method involving plastic matrix composites.

FSP is a unique non-joining method variant of FSW where it utilizes the stirring process to alter microstructure derived from FSW method to be super fine, modified with improved physical properties and at the same time suppressed defects such as porosity and short crack [34]. The introduction of foreign particle into base material during FSP creates new near quality to metal matrix composite or MMC structure and thus improving the material properties. This provides a new platform to produce improved future materials.

The consequent of FSP method emerges as a modified method of FB that allows bonding of overlapping thin plates through locally modified microstructure. The process utilizes less stirring effect due to the short pin geometry and thus differs from common FSW method.

The majority of these FSW variants stress on their ability to increase welding time and at the same time to reduce forces exerted from the welding process. The other purpose of these methods is to provide means of producing joining method involving different type of materials and configurations. More or less, these method share the same mechanism of mechanically manipulating soften work material and formation of fused material at the trailing edge.

3. Friction stir welding parameters

Independent process variables play significant effect on the welding process and the process control. The process variables entail the axial force for plunging, rotating tool rotational speed, rake angle, welding speed and tool geometry. The aforementioned variables strongly affect the heat generation rate, temperature profile within the work material, mechanical power required by the process, material evolution of the weldment and also loads distributed within the work material. These variables are extensively discussed in this chapter to understand the mechanics of joining, process and final weld properties optimizations, where direct measurement can be done experimentally and predicted numerically.

3.1. Effect of welding parameters on joint quality

It has been reported that rotational and traverse speeds have both direct and indirect influence to the final weldment. Its direct influences to the mechanics of joining suggesting the degree of stirring based on the contact condition and multi component loads. Whilst, it's indirect influences to mechanical properties of the weldment is heavily derived from the combination of temperature exposure and tool design [41]. Low rotational speed induces low stirring effect and finally low heat generation rate. At low traverse speed, it increases exposure to heat source, facilitate more material flow and reduced multi component loads, vice versa to high traverse speed but only to an extent. Extreme high rotational speed results too much heat while extreme high traverse speed results less heat, low stirring effect and increase travel resistance due to heavy loads on the rotating tool and hard work material at the leading edge. At this moment, the material is sheared to the lateral side instead of moving around the rotating tool direction [42]. Excessive heat which is generated from either high rotational speed or low traverse speed, or combination of both conditions, significantly reduces the mechanical properties of joint due to microstructure evolution of the regions exposed to excessive heat [43]. Albeit, the appropriate traverse and rotational speed below critical speeds might result optimum heat generation rate and reduced thermal exposure that produce good strength and hardness of weld joints [44, 45].

Torque produced during the welding process depends heavily on the contact conditions which are determined by the rotating tool rotational speed, degree of softness of work material or plasticity at the rotating tool to work material interface, axial load exerted and the tool design [22, 46, 47]. Any changes in the traverse speed at a constant tool rotational speed do not significantly affect the temperature profile compared to changes done in the rotational speed. These make the torque to be insensitive to the traverse speed. In addition, optimum rotating tool design influences torque produced through the effect of sum of contact areas and contact conditions at the interface where it plays major role in plastic deformation or strain work distribution, material transportation or flow and toward process loads and work material temperature [41, 48, 49, 50]. As temperature increases, work material temperature dependent shear stress plump and no longer display full solid properties thus reduces the torque at the rotating tool to work material interface and further reducing power and energy required to produce heat within the process.

3.2. Optimizing process parameters

Considerably vast works has been made in pursue to understand and optimize the physical process of FSW that influenced by the associated variables using both empirical as well as numerical models for the heat generation, material interaction and flow.

3.2.1. Thermal modelling

Heat generation is modelled based on the torque required to rotate a circular shaft relative to the material surface. The model is made by assuming a constant coefficient of friction, pressure distribution and 100% conversion of the shearing work to heat. It is also assumed that the net power required is directly proportional to the tool rotational speed and the tool shoulder radius i.e. $q \approx \omega R$ [51].

Friction work principle used for heat generation model is coupled with plastic work principle to model three-dimensional heat and material flow based on temperature dependent coefficient of friction and temperature dependent pressure distribution for aluminium alloys [26]. In detail, three-dimensional visco-plastic flow and heat transfer have been investigated through solving the equations of conservation of mass, momentum and energy by considering the heat source at two separate conditions. Firstly, visco-plastic flow and heat transfer at the tool to work material interface due to the mechanical friction or due to the plastic dissipation heat generation mechanisms and secondly, the visco-plastic flow and the heat transfer within the layers of soft work material away from the tool to work material interface under the combination of both friction and plastic dissipation heat generation mechanisms [11, 52, 53, 54].

The model is defined by the contact area, the radial distance of the rotating tool pin and shoulder, the material shear stress or the spatially variable coefficient of friction or their combinations, the angular velocity and the exerted normal pressure acted on the work material surface. Then, the model is validated through comparison of the computed heat generation, peak temperature and the total torque exerted on the tool with the experimental results. Contact conditions at the interface are described as sliding, sticking or partial sliding or sticking, known as slip factor is also being adapted. The slip factor is derived experimentally, determined by the plunge force and torque from the welding process. The slip factor yield a proportional relationship between plunge force and heat generation where Coulomb's law of friction is applied to describe the shear forces at the interface [10, 55]. Slip factor is also used to evaluate the welding energy and temperature, utilizing torque based heat input [53]. These works allow the prediction of the welding temperature from the transverse speed, tool rotational speed and the applied force. Ultimately, fully coupled thermo-mechanical model with adaptive boundary condition which applied both thermal and mechanical model is used to predict transient temperature profile, active developed stresses as well as the three-dimensional force components [13].

3.2.2. Model validation

The force and temperature measurement experiments are conducted under different welding parameters for model verification by differing the transverse and the tool rotational speed whilst maintaining the constant vertical force. The result is later used for the calculation of the heat input into the tool and workpiece. In relation, numerical model is developed to take account the process effects on the work material such as the material plasticity properties, thermal expansion and stress, cooling effect, stress stiffening, stress distribution, material strain, residual stress as well as the thermal history of the welding process [56, 57, 58].

The mechanical effect is visualised and simulate as material flow model to describe the process parametric effects on the soft work material flow and the welding mechanisms [59, 60]. The physical material flow highlights the particular material strain, its distribution and flow motion around the rotating tool, at the leading edge of advancing and retreating sides and at the trailing edge as well as the actual bond that might occur in the FSW process. Thus, thermo-mechanical model is required to exhibit the importance of the three-dimensional loads and torque exerted by the rotating tool material to determine the best and optimized parameter for the welding process of any materials which is greatly related to the joint and process properties such as residual stresses, process temperature, joint strength and productivity. The parameter optimization is related to variables such as welding speed, rotating tool rotational speed as well as rotating tool design. Proceeded, welding power has been modelled to determine the overall heat input for FSW process based on the traverse speed and tool rotational speed as well as its effect on the material properties. The model has been derived based on the relationship between the rotating tool rotational speed and the represented rotating tool torque with association to the key parameters aforementioned [61, 62].

Significantly all of these works and models represent the correlation of the mentioned independent variables of the associated welding parameters as well as material properties serve the heat generation, temperature distribution and joining mechanism that contribute to the success of the welding process. In summary, the relationship between the independent process variables and the dependent process output to the heat generation mechanisms is best described as in a closed and correlated system, explained by the interaction of process welding variables and key process conditions; physical, metallurgical, heat generation and heat transfer effect [63].

4. Mathematical modelling of welding forces & torque

FSW is not widely available in general application rather than conventional fusion joining methods especially in automotive industry due to shorter process and heat generation cycle. Thus, the true understanding of FSW process is still in far-reaching; understanding the physics and nature of the process, lacking of standards guideline and practice, optimization of the process for typical material usage or application as well as still typically not suitable for small scale robotic or manual handling. The mathematical model on the welding forces

and torque is proposed for optimizing FSW process and to study the effects of varying its parameters. The model is to be compared with experimental work [64, 65].

4.1. Model development & assumption

Initial heat generation takes place at the first contact of the rotational tool pin surface and continue throughout the plunging phase where the temperature distribution of the work material is asymmetrical at the leading, trailing edge as well as advancing and retreating side. It is based on the assumption that the interface heat generation is constant with the consideration of the constant rotating tool angular speed, ω , temperature-dependent pressure distribution function, $P(T)$, heat capacity, ρc_p , thermal conductivity, k and constant coefficient of friction, μ_k . Based on Fourier's 2nd law [66];

$$\rho c_p \frac{\partial T}{\partial t} = k \left(\frac{\partial^2 T}{\partial x^2} + \frac{\partial^2 T}{\partial y^2} + \frac{\partial^2 T}{\partial z^2} \right) + \dot{q} \quad (1)$$

Where ρc_p is the heat capacity, x , y , and z are the space coordinate and is the heat source term correspond to heat generated from the welding process. The function of the heat generation is directly related to friction work of the contacting surface thus accounts the sum of contact surface area of the tool. The sum or contact area is represented as function of rotating too plunge depth, h . The data used is as in table 1. Given;

$$A_{(h=0)} = \pi r_p^2 \quad (2)$$

$$A_{(0 < h < 5)} = A_{(h=0)} + \pi \left[\left(\frac{R_p}{h_p} h_{(0 \rightarrow 5)} + r_p \right) \left(\frac{R_p - r_p}{\sin 2} \right) - r_p S_2 \right] \quad (3)$$

$$A_{(h=5)} = A_{(0 < h < 5)} + \pi (R_s - R_p)^2 \quad (4)$$

For A is the contacting surface between the rotating tool and the work material surface, r_p is the bottom pin radius, R_p is the top pin radius, h_p is the total height of the pin and $\pi r_p S_2$ is the minor cone area.

Furthermore, the torque required to rotate the rotational tool relative to the static workpiece surface under $P(T)$ represents the conversion of mechanical work of the rotating tool. Given;

$$M = \int_0^{M_R} dM = \int_0^R \mu P(T) 2A(h) r dr = \mu P(T) A(h) R^2 \quad (5)$$

Or by simplification of the sum of contact area through cylindrical approximation, given [67, 68];

$$M = \int_0^{M_R} dM = \int_0^R \mu P(T) 2\pi r^2 dr = \frac{2}{3} \mu \pi P R^3 \quad (6)$$

Where M is the interfacial torque of the in contact workpiece surface and rotating tool surface, μ_k is the coefficient of friction, R is the contact surface radius, and $P(T)$ is temperature dependent pressure distribution across the interface.

For fully sliding contact condition and with assumption of all the friction work is converted into frictional heat, the average heat input per unit area and time becomes;

$$q_0 = \int_0^{M_R} \omega dM = \int_0^R \omega \mu P(T) 2\pi r^2 dr = \frac{2}{3} \omega \mu P R^3 = \frac{4}{3} \mu \pi^2 n P R^3 \quad (7)$$

Where q_0 is net power in Watt (Nms^{-1}) and ω is rotational speed (rads^{-1}). Apparently, in equation 7, heat input depends on the normal pressure distribution function, contact surface radius, temperature dependent function of coefficient of friction and the rotational speed of the rotating tool which produce transient heat generation, distributed into the work material and thus characterized the process variables for the friction stir welding process.

In order to understand the physics of the welding process in the expression of the mechanical loading associated to the welding process, a mathematical representation is derived based on figure 5;

$$r_1 = -(x_1 + x)i + y_1j - z_1k \quad (8)$$

$$r_2 = -(x_2 + x)i - y_2j - z_2k \quad (9)$$

$$r_3 = (x_3 - x)i - y_3j - z_3k \quad (10)$$

$$r_4 = (x_4 - x)i + y_4j - z_4k \quad (11)$$

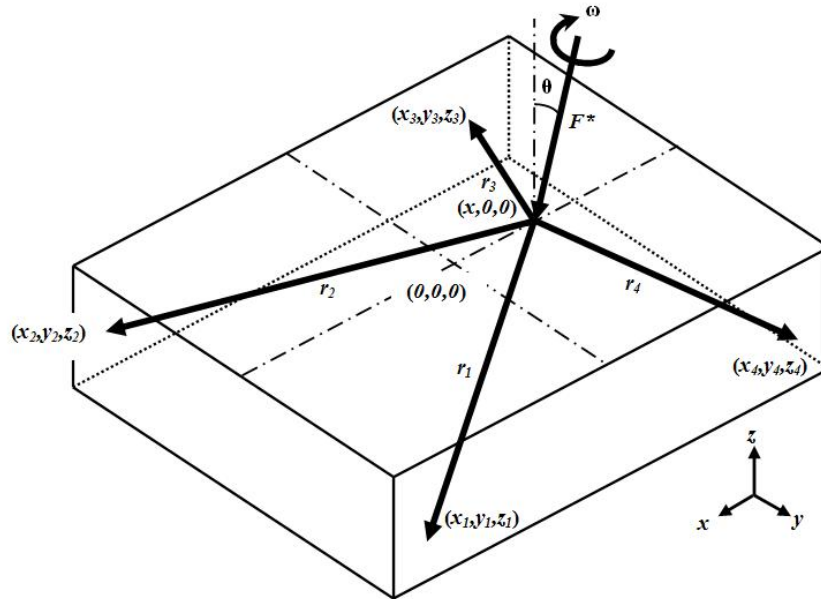


Figure 5. Free body diagram of multi-component load measuring device [65].

$$\sum F = 0 \quad (12)$$

$$F_{x,y,z}^* = \sum_{n=1}^4 Fn_{x,y,z} \quad (13)$$

$$F^* \sin \theta i + F^* \cos \theta k = (F_{1x}^* + F_{2x}^* + F_{3x}^* + F_{4x}^* - F_{1x} + F_{2x} + F_{3x} - F_{4x})i + (-F_{1y} - F_{2y} + F_{3y} - F_{4y})j + (F_{1z}^* + F_{1z} + F_{2z}^* - F_{2z} + F_{3z}^* - F_{3z} + F_{4z}^* + F_{4z})k \quad (14)$$

Where F^* , is the plunge force as the function of contact surface area and under the temperature dependent pressure distribution $P(T)$ for a desired depth of penetration. The torque exerted on the work material by the rotating tool mechanical friction work is calculated based on equation 6 and coupled by the moments reacted at each of the measuring references on the workpiece as in figure 5;

$$\sum M = 0 \quad (15)$$

$$M_{x,y,z}^* = \sum_{n=1}^4 rn_{x,y,z} \times Fn_{x,y,z} = 4(Rn_{x,y,z} \times Fn_{x,y,z}) \quad (16)$$

$$M_{x,y,z}^* = \frac{2}{3} \mu F_{x,y,z}^* R \quad (17)$$

Where;

$$M_1 = M_2 = M_3 = M_4 \quad (18)$$

$$r_1 \times F_1 = r_2 \times F_2 = r_3 \times F_3 = r_4 \times F_4 \quad (19)$$

In figure 5, the moment exerted on the measuring references is in equilibrium and the acting forces exerted by the rotational tool mechanism are determined from equation 18, generally;

$$\frac{1}{4} M_{x,y,z}^* = Rn_{x,y,z} \times Fn_{x,y,z} \quad ; n = 1, 2, \dots, 4 \quad (20)$$

$$r_n \times F_n = (y_n Fn_z + z_n Fn_y)i - (-x_n Fn_x)j + (-x_n Fn_y - y_n Fn_x)k \quad (21)$$

The general equation can be presented in a matrix form as;

$$\begin{bmatrix} \frac{1}{4} M_x^* \\ 0 \\ \frac{1}{4} M_z^* \end{bmatrix} = \begin{bmatrix} 0 & z_n & y_n \\ -z_n & 0 & x_n \\ -y_n & -x_n & 0 \end{bmatrix} \begin{bmatrix} Fn_x \\ Fn_y \\ Fn_z \end{bmatrix} \quad (22)$$

At any static equilibrium where the slip contact condition between the rotating tool and the workpiece surface remain constant, the moment at each of the measuring references remain

the same but dependent on the radius of the rotating tool and the function of pressure distribution $P(T)$ for the respective rotating tool position. The values for the moment are also remained constant at any Cartesian coordinate (x, y) location of the rotating tool on the surface of the workpiece. Although the basic assumption for the constant contact condition for the function of pressure distribution $P(T)$ in modelling the process is not physically correct but appropriate to be acceptable in the context of numerical model as average value used throughout the investigation.

Properties/parameter	Value
Work material dimension, mm	200 X 200 X 7
Shoulder radius, mm	9
Tool radius, mm	3
Pin radius, mm	2.852
Pin height, mm	5
Pin conical angle, °	2
Tool angle, °	2
Workpiece material	6061 T-6
Tool material	M42
Coefficient of friction	Figure 7
Plunge forces	Figure 8

Table 1. Summary of data used for loads and torque calculation [5].

4.1.1. Co-planar analysis

A closer approximation is made on the geometry of the work material is to measure the reaction forces and moment caused by the rotating tool from the friction welding process. Equation 22 is reduced by performing co-planar analysis at measuring points of the workpiece as in figure 6 for the initial heat generation until the full penetration of the stirrer tool.

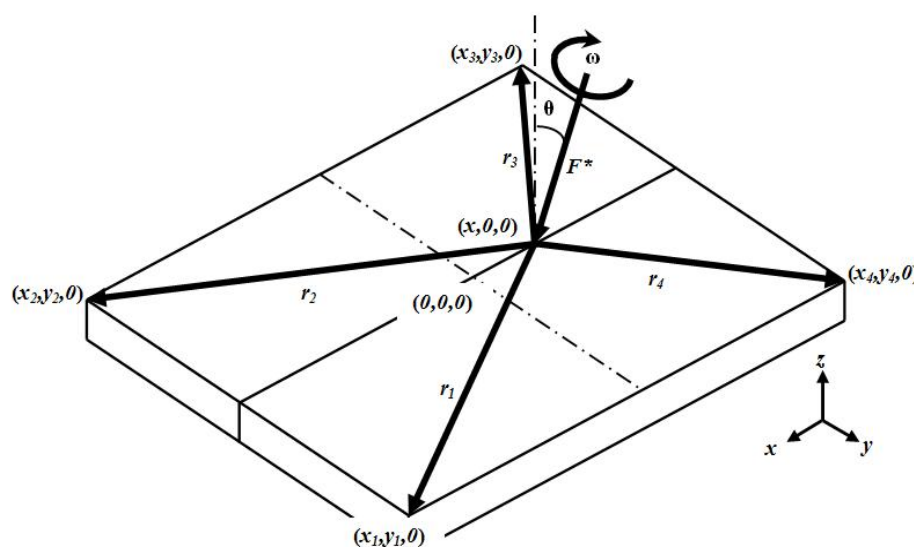


Figure 6. Co-planar analysis of the workpiece material during welding process [65].

Parametric analysis are carried out based on the work material temperature dependent tensile, yield and shear strengths properties, welding configuration, work material dimension and also tool design to investigate loads and torque distributed within the work material. The temperature dependent material properties data used in the calculation are as in figure 7 and 8 used to determine the theoretical plunge forces for the FSW process. In addition, a constant plunge force is proposed as to simulate the experimental work as comparison to numerical analysis.

Theoretically in this work, the mechanical properties suggest the controlling parameters of the welding process especially regarding the plunge force which is based on the contact area and controlled pressure parameter on the tool, heat energy consumed and the mechanical loads applied.

The details of the parametric analysis are explained based on the case studies as carried as;

Case 1: Theoretical plunge force based on temperature dependent tensile strength. This approach is based on the assumption that contact condition is fully sliding follows the temperature dependent coefficient of friction curve as in figure 7.

Case 2: Theoretical plunge force based on temperature dependent yield strength. This approach is also based on the assumption that contact condition is fully sliding.

Case 3: Theoretical plunge force based on temperature dependent shear strength. The assumption for fully sticking contact condition is that the rotating tool which is trusting and work material is separated by a thin layer of plasticised material at the contact interface.

Case 4: Experimental plunge force based on manual force and plunge depth control method [5]. Force and plunge depth control methods are common control method for FSW process [69, 70].

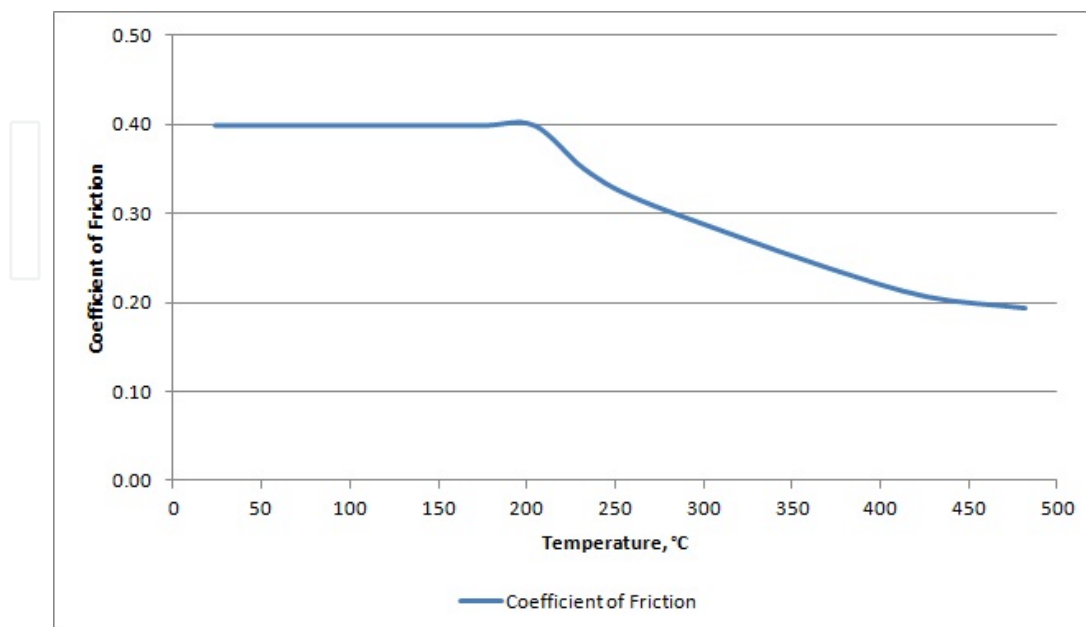


Figure 7. Temperature dependent coefficient of friction [5].

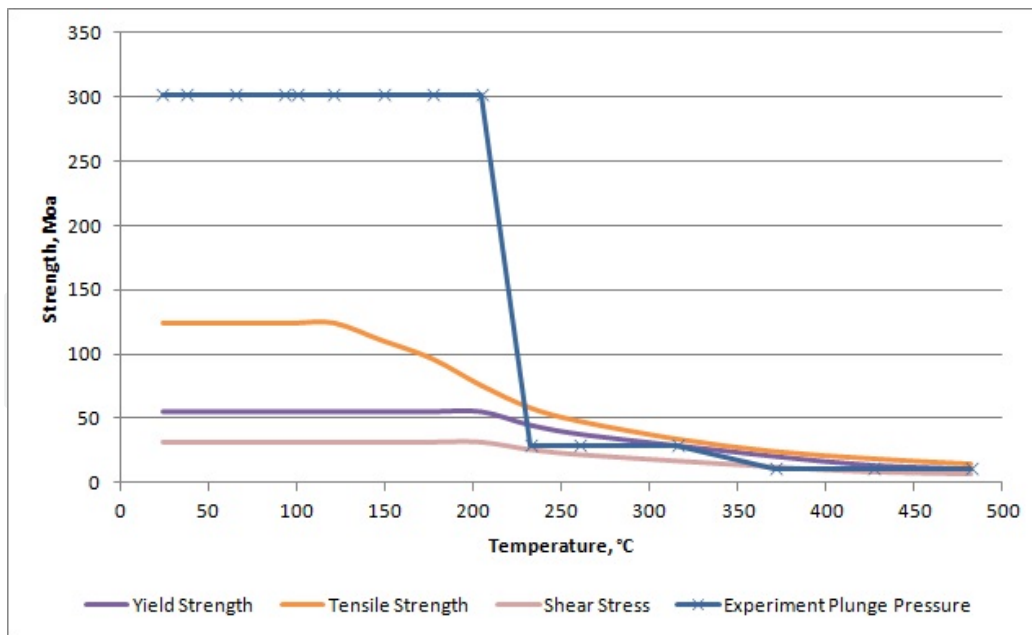


Figure 8. Variable temperature dependent material properties of aluminium alloy 6061 and plunge pressure variation for FSW process cases 1 – 4 [5, 6].

Though in this work, only case 1, 3 and 4 are being considered to visualize the maximum and minimum limits of the parametric effect in comparison to the experimental work. Case 1 encompasses the maximum strength value of the work material prior failure due to the mechanical effect of the FSW process. As for case 3, it represents the minimum requirement of the FSW process to initiate mechanical or physical effect on the work material. Finally, case 4 is the corresponding load suggested based on the work holding fixture as in figure 1 [5, 65].

4.2. Model validation with experimental data

The plunge variation profiles in FSW processes based on the temperature dependent work material properties and experimental plunge pressure value are as exhibited in figure 8. It is noticeable that the cases are significant at temperature range approximately 120°C to 220°C, where the theoretical plunge pressure started to decrease. The work material becomes soft and lost its strength, allowing the rotating tool to displace axially into the work material. The corresponding rotating tool plunge force theoretical calculation based on the plunge pressures schemes aforementioned are compared to experimental result and exhibited in figure 9.

During the plunging phase, the rotating tool thrusting under the plunge pressure profiles and constant rotational speed produces mechanical torque. It acts on the work material and initiates the mechanical friction work thus results the friction heat. The variations of mechanical torque exerted at the rotating tool and the work material interface during the plunging phase are as in figure 10.

Sticking and sliding contact conditions referred as case 1 and 3, exhibit significant torques built up beyond 300°C. For case 4, high torque exerted at initial plunge phase abruptly

decrease as the temperature approaches 220°C before it increase back at temperature beyond 300°C. The decrease in torque indicate the softening effect of the work material while the immediate increase of the torque values are due to the rotating tool shoulder surface comes into contact to the work material.

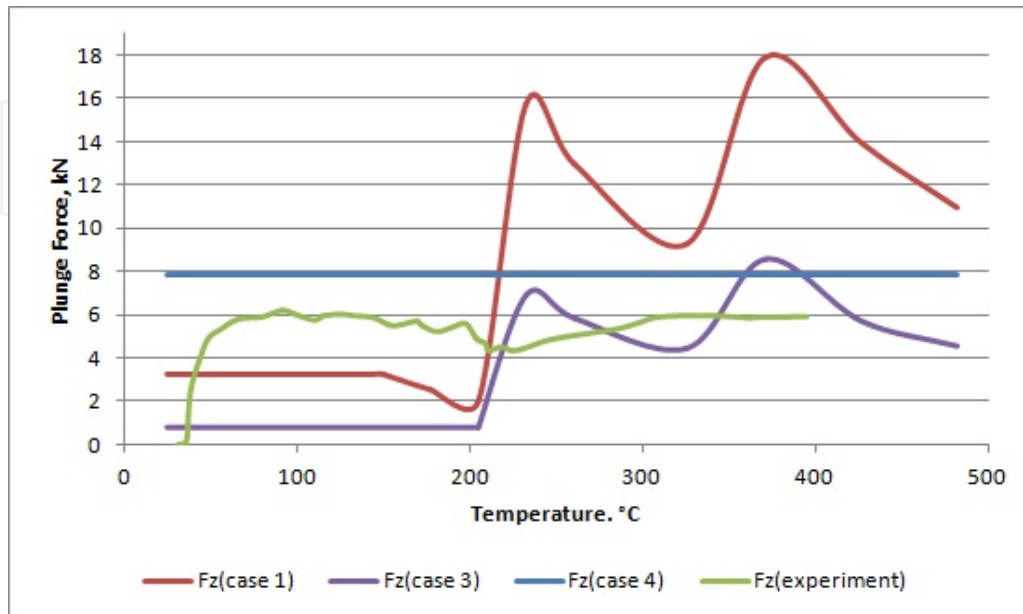


Figure 9. FSW plunge forces as controlling parameters [5].

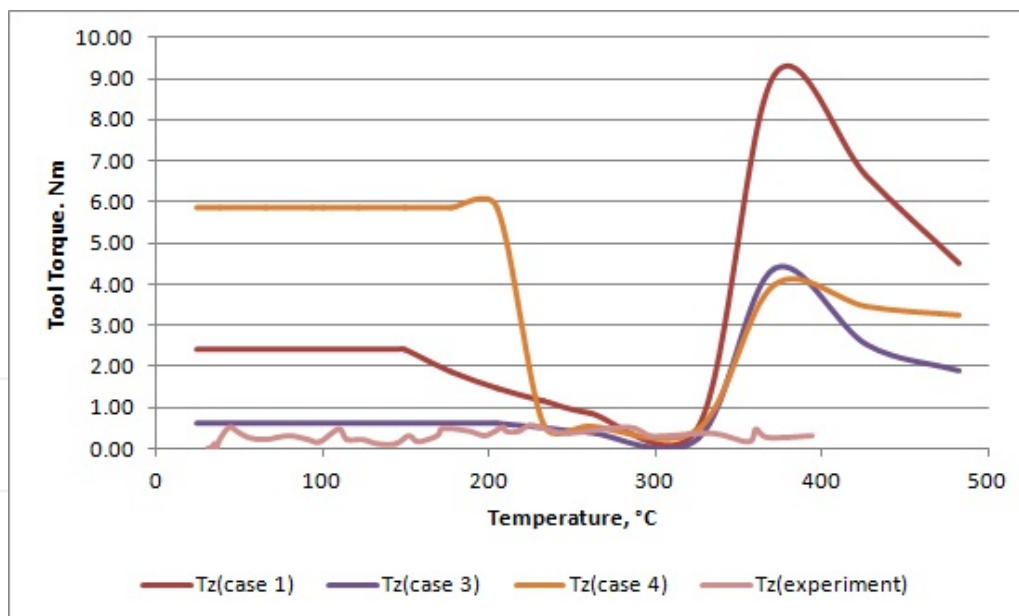


Figure 10. Tool torque exerted at the tool - work material interface for case 1, 3 & 4 [5].

An approximation of the process is based on case 4 where plunge pressure is based on manual control of constant plunge force. The comparison of the theoretical plunge forces and experimental work of the FSW process reveal distinct variation based on the assumption used. However, the values act as references for the actual FSW process that agree to the experimental result as shown in figure 9. The experimental result shows that its

profile is approximate to case 4 plunge force scheme only at lower value. As for the rotating tool torque, the experimental value remains closed to the value exerted by case 3 scheme at almost constant trend. It described the nature of material in respond to the heat and mechanical friction during the FSW process.

5. Conclusion

FSW process benefits solid state joining method that has great advantage on light weight material such as aluminium alloy due to its thermal properties which make it difficult to be joined using conventional methods. Similarly to the other welding method, heat generation and heat transfer play major role in determining the success of the joining process as well as predominantly establish the joint characteristics and properties. Though the detail of the process mechanism and the effect on the welding has been widely studied in lab scale, good understanding of the process mechanism provides a better view on choosing the best parameter for the process and finally to achieve the best result in practice.

The future outlook of the process is very promising with new interest on its recent development that allows broader application in term of material used as well as process improvement. In addition, the development of mathematical analysis provides the ability to predetermine the effect of parametric study of the process effect on the work material at a shorter time as well as to be adapted to process automation.

Author details

Jauhari Tahir Khairuddin and Jamaluddin Abdullah

School of Mechanical Engineering, Universiti Sains Malaysia, Nibong Tebal, Penang, Malaysia

Zuhailawati Hussain

School of Materials and Mineral Resources Engineering, Universiti Sains Malaysia, Nibong Tebal, Penang, Malaysia

Indra Putra Almanar

Mechanical Engineering Department, Universiti Teknologi Mara, Permatang Pauh, Penang, Malaysia

Acknowledgement

This present work is supported by Universiti Sains Malaysia through RU-Grant (814084), Universiti Sains Malaysia Institute of Postgraduate Studies Graduate Research Fund (IPS-GRF) and USM-Fellowship scheme, which are greatly acknowledged.

6. References

- [1] Thomas WM, Nicholas ED, Needham JC, Murch MG, Templesmith P, Dawes CJ. Friction Stir Butt Welding, GB Patent No. 9125978.8; 1991.

- [2] Dawes CJ, Thomas WM. Friction Stir Welding of Aluminium Alloys. *TWI Bulletin*; 1995; 6 : 124-127.
- [3] Hwang YM, Kang ZH., Chiou YC, Hsu HH. Experimental Study on Temperature Distributions Within the Workpiece During Friction Stir Welding of Aluminium Alloy. *Int J of Mach Tools Manu*; 2008; 48 : 778-787.
- [4] Kim D, Badarinarayan H, Kim JH, Kim C, Okamoto K, Wagoner RH, Chung K. Numerical Simulation of Friction Stir Butt Welding Process for AA5083-H18 Sheets. *Eur J Mechanics A-Solid*; 2010; 29 (2) : 204 – 215.
- [5] Jauhari TK. Development of Multi-Component Device for Load Measurement and Temperature Profile for Friction Stir Welding Process [M.Sc Thesis]. Penang: Universiti Sains Malaysia; Unpublished. 2012.
- [6] American Welding Society. *Welding Handbook*, 9th Edition, Volume 3: Welding Process; AWS; 2007.
- [7] Popov VL. *Contact Mechanics and Frictions: Physical Principal and Application*. London: Springer; 2010.
- [8] Sherwood BA, Bernard WH. Work and Heat Transfer in the Presence of Sliding Friction. *Am J Phys*. November 1984; 52 (11) : 1001-1007.
- [9] Ravichandran G, Rosakis AJ, Hodowany J, Rosakis P. On the Conversion of Plastic Work Into Heat During High-Strain-Rate Deformation. *Shock Compression of Condensed Matter Meeting*. American Physical Society; June 24-29, 2001 . p 557 – 562.
- [10] Schmidt H, Hattel J, Wert J. An Analytical Model for the Heat Generation in Friction Stir Welding. *Model Simul Mater Sc*. 2004; 12 (1) : 143-157.
- [11] Nandan R, Roy GG, DebRoy T. Numerical Simulation of Three-Dimensional Heat Transfer and Plastic Flow During Friction Stir Welding. *Metal Mater Trans A*. April 2006; 34A : 1247 – 1259.
- [12] Schmidt HB, Hattel JH. Thermal Modelling of Friction Stir Welding. *Scripta Mater*. 2008; 58 : 332 – 337.
- [13] Soundararajan V, Zekovic S, Kovacevic R. Thermo-Mechanical Model With Adaptive Boundary Conditions for Friction Stir Welding AL 6061. *Int J Mach Tool Manu*. 2005; 45 (14) : 1577-1587.
- [14] Schneider J, Beshears R, Nunes Jr. AC. Interfacial Sticking and Slipping in the Friction Stir Welding Process. *Mat Sci Eng A*. 2006; 435 – 436 : 297 – 304.
- [15] Colligan KJ, editors. *Friction Stir Welding: From Basic to Applications – 2. The Friction Stir Welding Process: An Overview*. CRC Press; 2010. p 15 – 38.
- [16] Khandkar MZH, Khan JA. Thermal Modelling of Overlap Friction Stir Welding for Al-Alloys. *J Mater Process Manuf Sci*. 2001; 10 (2) : 91 – 105.
- [17] Schmidt H, Hattel J. Modelling Heat Flow Around the Tool Probe in Friction Stir Welding. *Sci Technol Weld Joining*. 2005; 10 (2) : 176 – 186.
- [18] Khandkar MZH, Khan JA, Reynolds AP. In: *Prediction of Temperature Distribution and Thermal History During Friction Stir Welding: Input Torque Based Model*. *Sci Technol Weld Joining*. 2003; 8 (3) : 165 – 174.

- [19] Song M, Kovacevic R. Thermal Modelling of Friction Stir Welding in A Moving Coordinate System and its Validation. *Int J Mach Tools Manuf.* 2003; 43 : 605 – 615.
- [20] Shi QY, Dickerson T, Shercliff HR., Thermo-mechanical Finite Element Modelling in Friction Stir Welding of AL – 2024 Including Tool Loads. In: *Proceeding of the 4th International Symposium on Friction Stir Welding.* 2003.
- [21] Nandan R, DebRoy T, Bhadeshia HKDH. Recent Advances in Friction Stir Welding – Process, Weldment Structure and Properties. *Prog Mater Sci.* 2008; 53 : 980 – 1023.
- [22] Arora A, Nandan R, Reynolds AP, DebRoy T. Torque, Power Requirement and Stir Zone Geometry in Friction Stir Welding Through Modelling and Experiments. *Scripta Mater.* 2009; 60 : 13 – 16.
- [23] Arora A, Zhang Z, De A, DebRoy T. Strains and Strain Rates during Friction Stir Welding. *Scripta Mater.* 2009; 61 : 863 – 866.
- [24] Jata KV, Semiatin SL. Continuous Dynamic Recrystallization During Friction Stir Welding of High Strength Aluminium Alloys. *Scripta Mater.* 2008; 43 (8) : 743 – 749.
- [25] Song M, Kovacevic R. Numerical and Experimental Study of the Heat Transfer Process in Friction Stir Welding. In: *Proceedings of the Institution of Mechanical Engineers, Part B: J Eng Manu.* 2003; 217 (1) : 73 – 85.
- [26] Dong P, Lu F, Hong JK, Cao Z. Coupled Thermomechanical Analysis of Friction Stir Welding Process Using Simplified Models. *Sci Technol Weld Joining.* 2001; 6 (5) : 281-287.
- [27] Elangovan K, Balasubramanian V, Babu S. Developing an Empirical Relationship to Predict Tensile Strength of Friction Stir Welded AA2219 Aluminium Alloy. *J Mater Eng Perform.* 2008; 17 (6) : 820 – 830.
- [28] Moreira PMGP, Santos T, Tavares SMO, Richter-Trummer V, Vilaca P, de Castro PMST. Mechanical and Metallurgical Characterization of Friction Stir Welding Joints of AA6061-T6 with AA6082-T6. *Mater Design.* 2009; 30 : 180 – 187.
- [29] Tutum CC, Hattel JH. Optimisation of Process Parameters in Friction Stir Welding Based on Residual Stress Analysis: A Feasibility Study. *Sci Technol Weld Joining.* 2010; 15 (5) : 369 – 377.
- [30] Smith C, Hinrichs J, Crusan W. Robotic Friction Stir Welding: The State-of-the-Art. In: *Proceeding of the 4th International Friction Stir Welding Symposium.* Salt Lake City, UT; May 2003.
- [31] Kumagai M, Tanaka N. Application of friction stir welding to welded construction of Aluminum alloys. *J Light Met Weld Constr.* 2001; 39 : 22-28.
- [32] Kallee SW, John D, Nicholas ED. Railway Manufacturers Implement Friction Stir Welding. *Weld J.* 2002; 81 (10) : 47 – 50.
- [33] Delany F, Kallee SW, Russell MJ. Friction Stir Welding of Aluminium Ships. In: *International Forum on Welding Technologies in the Shipping Industry.* Shanghai, China; June 2007.
- [34] Arbogast WJ. Friction Stir Welding – After a Decade of Development. *Weld J.* 2006; (3) : 28 – 35.

- [35] Kallee SW, Kell JM, Thomas WM, Wiesner CS. Development and Implementation of Innovative Joining Process in The Automotive Industry. In: DVS Annual Welding Conference. Essen, Germany; September 2005.
- [36] ESAB. Friction Stir Welding – the ESAB Way, XA00123720 [Internet]. 2004 [cited 24 May 2012]. Available from:
http://www.esab.co.kr/esab/mc_data/pdf/Friction%20Stir%20Welding.pdf
- [37] Nunes AC. Friction Stir Welding. In: Schwart MM, Innovation in Materials Manufacturing, Fabrication, and Environmental Safety, Boca Raton, FL . CRC Press. 2011: 88 – 119
- [38] Ding J, Carter R, Lawless K, Nunes AC, Russell C, Suits M. Friction Stir Welding Flies High at NASA. *Weld J*. 2006; 85 (3) : 54 – 60.
- [39] Gerlich A, North T. Friction Stir Spot Welding of Aluminum Alloys. *Canadian Weld Assoc J, IIW Special Ed*. 2006; 57 – 58.
- [40] Mishra RS, Ma ZY. Friction Stir Welding and Processing. *Mat Sci Eng*. 2005; 50 (1-2) : 1-78.
- [41] Elangovan K, Balasubramanian V. Influences of Tool Pin Profile and Tool Shoulder Diameter on the Formation of Friction Stir Processing Zone in AA6061 Aluminium Alloy. *Mater Design*. 2008; 29 : 362 – 373.
- [42] Zhang Z, Liu YL, Chen JT. Effect of Shoulder Size on the Temperature Rise and the Material Deformation in Friction Stir Welding. *Int J Adv Manuf Tech*. 2009; 45 : 889 – 895.
- [43] Liu HJ, Shen JJ, Huang YX, Kuang LY, Liu C, Li C. Effect of Rotation Rate on Microstructure and Mechanical Properties of Friction Stir Welded Copper. *Sci Technol Weld Joining*. 2009; 14 (6) : 577 – 583.
- [44] Ren SR, Ma ZY, Chen LQ. Effect of Welding Parameters on Tensile Properties and Fracture Behavior of Friction Stir Welded Al-Mg-Si Alloy. *Scripta Mater*. 2007; 56 : 69 – 72.
- [45] Patil HS, Soman SN. Experimental Study on the Effect of Welding Speed and Tool Pin Profiles on AA6082-O Aluminium Friction Stir Welded Butt Joints. *Int J Eng Sci Technol*. 2010; 2 (5) : 268 – 275.
- [46] Zhang Z, Zhang HW. Numerical Studies on the Effect of Transverse Speed in Friction Stir Welding. *Mater Design*. 2009; 30 : 900 - 907
- [47] Cui S, Chen ZW, Robson JD. A Model Relating Tool Torque and Its Associated Power and Specific Energy to Rotation and Forward Speed During Friction Stir Welding/Processing. *Inter J Mach Tools Manuf*. 2010; 50 : 1023 – 1030.
- [48] Buffa G, Hua J, Shivpuri R, Fratini L. Design of Friction Stir Welding Tool Using the Continuum Based FEM Model. *Mater Sci Eng A*. 2006; 419 : 381 – 388.
- [49] Hattingh DG, Blignault C, van Niekerk TI, James MN. Characterization of the Influences of FSW tool Geometry on Welding Forces and Weld Tensile Strength Using an Instrumented Tool. *J Mater Process Technol*. 2008; 230 : 46 – 57.
- [50] Arora A, De A, DebRoy T. Toward Optimum Stir Welding Tool Shoulder Diameter: *Scripta Mater*. 2011; 64 : 9 – 12.

- [51] Frigaard Ø, Grong Ø, Midling OT. A Process Model for Friction Stir Welding of Age Hardening Aluminum Alloys. *Metall Mater Trans A*. May 2001; 32 (5) : 1189-1200.
- [52] Buffa G, Hua J, Shivpuri R, Fratini L. A Continuum Based FEM Model for Friction Stir Welding – Model Development. *Mater Sci Eng A*. 2006; 419 : 389 – 396.
- [53] Nandan R, Roy GG, Lienert TJ, DebRoy T. Three-Dimensional Heat and Material Flow During Friction Stir Welding of Mild Steel. *Acta Mater*. 2007; 55 : 883 – 895.
- [54] Ulysse P. Three-Dimensional Modeling of the Friction Stir-Welding Process. *Int J Mach Tools Manuf*. 2002; 42 : 1549-1557.
- [55] Colegrove PA, Shercliff HR, Zettler R. Model for Predicting Heat Generation and Temperature in Friction Stir Welding From the Material Properties. *Sci Techno Weld Joining*. 2007; 12 (4) : 284-297.
- [56] Chen, CM, Kovacevic, R. Thermomechanical Modeling and Force Analysis of Friction Stir Welding by Finite Element method. In: *Proceeding of the Institution of Mechanical Engineers, Part C. J Mech Eng Sci*. 2004; 218 : 509-519.
- [57] Hamilton C, Dymek S, Sommer. A Thermal Model for Friction Stir Welding in Aluminum Alloys. *Int J Mach Tool Manuf*. 2008; 28 : 1120-1130.
- [58] Chen CM, Kovacevic R. Parametric Finite Element Analysis of Stress Evolution During Friction Stir Welding. In: *Proceeding of Institute of Mechanical Engineers Part B. J Manuf*. 2006; 22 (28) : 1359 – 1371.
- [59] Fratini L, Buffa G, Palmeri D, Hua J, Shivpuri R., Material Flow in FSW of AA7075 – T6 Butt Joints: Numerical Simulations and Experimental Verifications. *Sci Technol Weld Joining*. 2006; 11 (4) : 412 – 421.
- [60] Zhang W, Zhang Z, Chen JT. 3D Modeling of Material Flow in Friction Stir Welding Under Different Process Parameter. *J Mater Process Techn*. 2007; 183 : 62-70.
- [61] Pew JW, Record JH, Nelson TW, Sorensen CD. Development of A Heat Input for Friction Stir Welding. In: *ASM proceeding of International Conference: Trends in Welding Research*. 2005: 247 – 251.
- [62] Pew JW. A Torque-Based Weld Power Model for Friction Stir Welding [Msc thesis]. Brigham Young University; December 2006.
- [63] Colligan KJ, Mishra RS. A Conceptual Model for The Process Variables Related to Heat Generation in Friction Stir Welding of Aluminum. *Scripta Mater*. 2008; 58 : 327 – 331.
- [64] Benedyk JC: *Aerospace Structural Metals Handbook – Nonferrous Alloys*; CINDAS LLC. 2008: 68.
- [65] Jauhari TK, Indra PA, Zuhailawati H. Mathematical Model for Multi Component Forces & Torque Determination in Friction Stir Welding. *Adv Mater Res*. 2011; 230-232 : 1255 - 1259.
- [66] Incropera, DeWitt: *Fundamentals of Heat and Mass Transfer*, 2th Edition; Singapore; Wiley. 1990.
- [67] Midling OT, Grong Ø. A process model for friction welding of Al-Mg-Si alloys and Al-SiC metal matrix composites; 1: HAZ temperature and strain rate distribution. *Acta Metall Mater*. 1994; 42 : 1595-1609.
- [68] Crossland B. Friction Welding. *Contemporary Physics*. 1971; 12 (6) : 559-574.

- [69] Longhurst WR, Strauss AM, Cook GE. Enabling Automation of Friction Stir Welding: The Modulation of Weld Seam Input. *J Dyn Sys Meas Control*. 2010; 132: 1-11.
- [70] Davis TA, Shin YC, Yao B., Observer-Based Adaptive Robust Control of Friction Stir Welding Axial Force. *IEEE-ASME Trans Mechatron*. 2011; 16 (6) : 1032-1039

IntechOpen

IntechOpen